Ballistic quantum transport study of Al contacting silicane using empirical pseudopotentials

Peter D. Reyntjens[1,2], Maarten L. Van de Put[1] and William G. Vandenberghe[1]

[1] Department of Materials Science and Engineering, The University of Texas at Dallas

[2] Department of Material Engineering, KULeuven, Belgium

Abstract—We use a plane-wave based quantum transport approach to model the properties of metal contacts to two-dimensional (2D) semiconductors. Using the example of Al contacted to silicane, we show that our model is capable of obtaining the carrier density, potential distribution and current flow at the atomistic level. We self-consistently calculate the current density in an Al-silicane contact and show that the current mainly flows through the edge of the contact as opposed to being distributed along the entire length of the contact region. We find a contact resistance of $3.8 \cdot 10^4 \Omega\mu$m; a high value which we attribute to the large difference between the Al work function and the silicane electron affinity.

Index Terms—Quantum transport, empirical pseudopotentials, contact resistance, two-dimensional materials

I. INTRODUCTION

In the search for optimal gate control over the channel of field-effect transistors, the body thickness of the semiconductor has been reduced to the atomic scale. Two-dimensional (2D) materials, such as MoS_2, are strong candidates for future technology nodes. However, when contacting 2D semiconductors with a metal, large contact resistances are observed [1]. To better understand the factors at the atomistic scale, we perform self-consistent quantum mechanical transport simulations using empirical pseudopotentials.

There exists a wide range of simulation methods that provide insight into the properties of metal-2D semiconductor contacts. A semi-classical Schottky barrier model [2], [3] based on Landauer's formalism provides insight at the device level. Banerjee *et al.* [4] investigated the effect of surface roughness on the quality of metal/MoS_2 contacts using a self-consistent transmission line model. *Ab-initio* methods provide a deeper insight into the nature of the contact interface [5]. Pan *et al.* investigated the interfaces between various metals and monolayer MoS_2 using Density Functional Theory (DFT) and the non-equilibrium Green's function (NEGF) method. Luisier *et al.* [6] employed a combination of DFT, Maximally Localized Wannier Functions (MLWF) and the NEGF formalism to investigate the electronic transport through metal/MoS_2 interfaces.

Here we present Al on silicane as an example heterostructure to investigate the transport characteristics of metal-2D semiconductor contacts using an in-house plane-wave based method [7]. Using our model, we have access to the real-space carrier density and are able to model current flow at an atomistic level.

II. METHOD

A. DFT: Interlayer distance

Figure 1 shows the unit cell used in the simulation of our Al-silicane contact heterostructure. Because of the lattice mismatch, the commensurate unit cell is quite large when we leave both materials unstrained. We apply a strain of 21% to the silicane layer, while leaving the Al unstrained, in order to obtain a unit cell which allows for computationally feasible calculations.

To obtain the correct distance between the Al and the silicane, we perform a relaxation of the structure, while keeping the lattice constant the same. For the structural relaxation, we use Density Functional Theory as implemented in the Vienna Ab-initio Simulation Package (VASP). The resulting distance between Al and silicane is 2.44Å. We use the DFT calculated interlayer distance in all subsequent calculations.
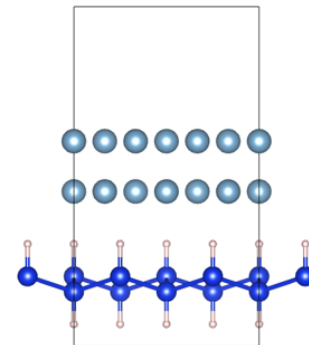

Fig. 1: The commensurate unit cell used for the Al-silicane contact calculations. The Al (top) has an FCC (111) surface facing the silicane (bottom).

B. Contact heterostructure

Figure 2 shows the structure of our Al-silicane contact. We take three separate regions into account: *Region I*, where there is only Al, *Region II*, where the Al is on top of a silicane layer, and *Region III*, where only the silicane is present. Following the preparation of the structure, we take care to properly calculate the properties of the two materials.

We use the Empirical Pseudopotential Method (EPM) [8] to calculate the band structures of silicane and Al. The EPM parameters have been optimized by Laturia *et al.* to accurately
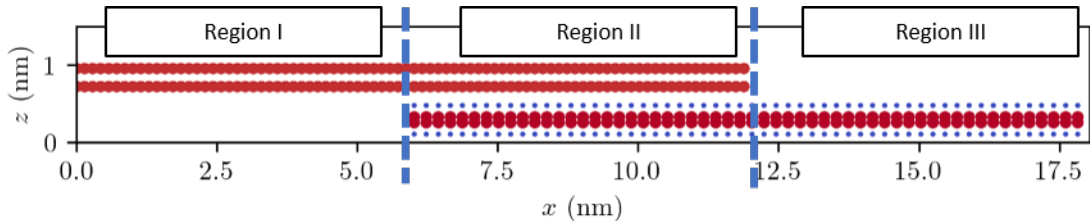
Fig. 2: The structure of our Al-silicane contact. The simulation is comprised of three different regions: *Region I*, where only the Al is present, *Region II*, where the Al and silicane are present, and *Region III*, where only the silicane is present.

produce band structures obtained using DFT [9]. In the case of Al, the parameters were optimized using the gerneralized gradient approximation as proposed by Perdew, Burke and Ernzerhof (PBE) [10]. The silicon EPM parameters were obtained the silicon DFT band structure, calculated using Hybrid Functionals to account for the well-known band gap underestimation for semiconductors by standard DFT methods [11].

The EPM parameters for both materials are then used by our in-house Plane-wave Electron TRAnsport (PETRA) solver [7] to calculate the eigenstates of the commensurate unit cell of Fig. 1. For computational efficiency, the PETRA code uses a Bloch wave basis set, which is the same across the entire simulation domain. Specifically, the Bloch wave basis set associated with the Al + silicane heterostructure of Fig. 1 is used throughout the entire structure. The difference between the different regions of the structure, Fig. 2, is made by obtaining the difference between the original potential of the supercell of Fig. 1 and a local atomic potential. To make sure that the materials are correctly simulated across the three regions of the simulation domain (see Fig. 2), we reconstruct the band structures of the Al and the silicane at the left and right edges of the simulation domain, respectively. We find that the Bloch wave basis, in combination with the local atomic potentials, accurately reconstructs the band structures across the different regions of the simulation domain.

C. Self-consistent calculations

Once the structure is ready, we use the PETRA solver to self-consistently calculate the properties of the contact. We apply an n-type doping of $2 \cdot 10^{13}$ cm^{-2} to the silicane layer. We first self-consistently calculate the potential and charge distribution in the unbiased (equilibrium) case, and subsequently apply a bias of -0.1 eV over the structure and again perform a self-consistent calculation. From the current through the contact at -0.1 eV, we extract the contact resistance.

III. RESULTS AND DISCUSSION

Figure 3 (right) shows the transmission through the structure, in the biased case. Figure 3 (left) shows the self-consistently calculated potential ϕ_{Al} in the Al, taken along a cutline at $z = 0.73$Å, and shifted by the Al workfunction, and the conduction and valence bands of silicane, taken along
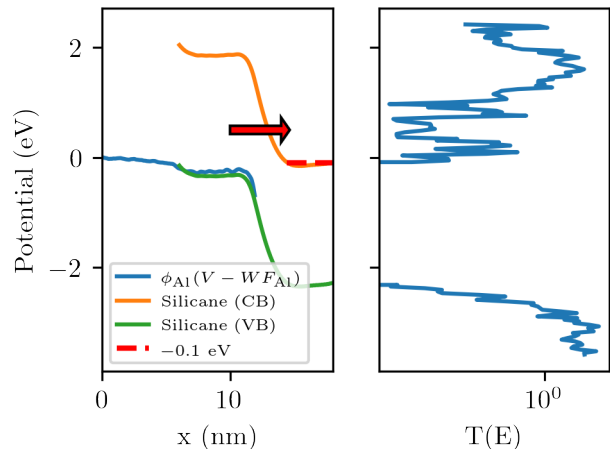

Fig. 3: (Left) Band diagram showing the silicane conduction and valence bands, and the potential in the metal, ϕ_{Al} is shifted by the work function (V - WF). We have applied a 0.1 eV bias over the structure. The red arrow indicates the tunneling path taken by the charge carriers in the biased contact. (Right) Semilog plot of the transmission through the device, adjusted to place the conduction band of silicane at the bias level.

a cutline at $z = 0.39$Å and shifted by the silicane electron affinity, when the bias is applied. The arrow indicates that the current is most likely to flow close to the edge of the contact, where the Al potential and silicane conduction band are closest to each other.

Figure 4 shows the self-consistently calculated free charge density in the structure. The free charge density in the Al forms a standing wave pattern with a free charge density that oscillates above (red) and below (blue) the Fermi level. We attribute the standing wave pattern to a high degree of reflection at the edge of the Al slab in combination with external scattering processes. We observe that the originally n-type doped silicane is completely inverted below the Al.

Figure 5 uses a log plot to show the current density in our structure, when the bias of -0.1 eV is applied. The current increases exponentially from the left side of the contact region (*Region II*) to the edge of the contact region, at the edge of the Al. We attribute the edge-concentrated current flow to the large contact resistance of $3.8 \cdot 10^4$ Ωµm that is formed when the Al
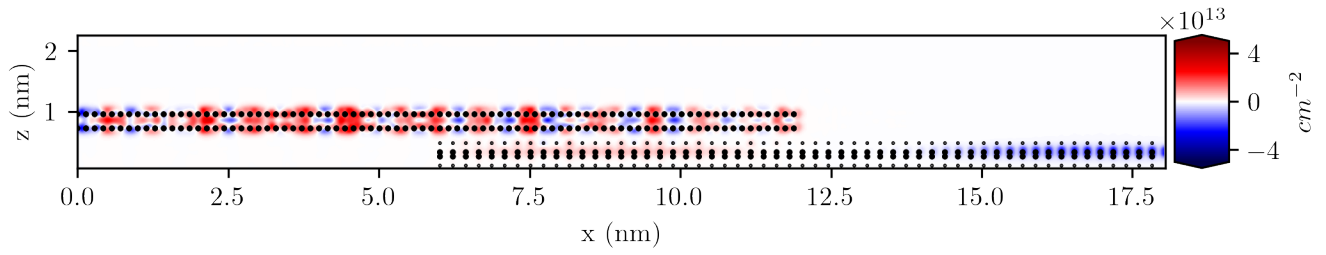
Fig. 4: The self-consistently calculated free charge density in the structure. Holes (positive charge) are shown in red, while electrons (negative charge) are shown in blue.
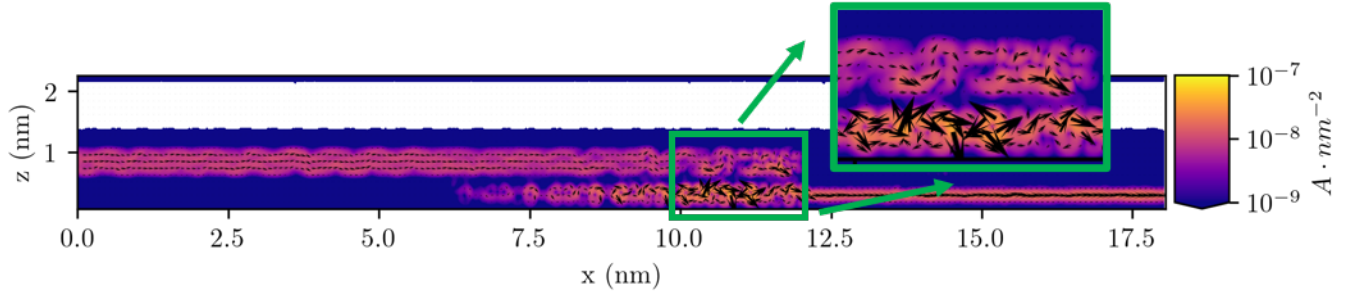

Fig. 5: The current density through the structure. The current density is represented using a vector plot, with arrows indicating the value and direction of the current density. The colormap shows the absolute value of the current density at each point on a logartihmic scale.

inverts the originally n-type silicane upon contact formation. Silicane has a very low electron affinity (2.19 eV), which, in combination with the Al workfunction of 4.2 eV forms a large Schottky barrier at contact and inverts the silicane below the Al. Due to the Schottky barrier, a large contact resistance forms and injection at the edge of the Al is promoted over area-dependent injection.

Using systems with a smaller difference between the metal work function and the semiconductor electron affinity, such as Al and MoS_2 ($\chi = 4.2$ eV), would reduce the Schottky barrier and reduce the edge-dependence of the current flow. However, other factors are important as well. As Szabó *et al.* [6] point out, the penetration of the metal wavefunction into the semiconductor bandgap has a significant impact on the current flow between the two materials.

IV. CONCLUSIONS

We have applied the PETRA solver to metal-semiconductor contacts and studied the properties of Al on silicane as an example system. We performed self-consistent calculations to obtain the potential, charge distribution and current density through the contact. The contact resistance of $3.8 \cdot 10^4 \Omega \mu$m was found to be due to the large difference between the Al work function and the silicane electron affinity. The mismatch between the Al and silicane band structures causes an inversion of the carrier density in the silicane layer below the Al.

Our model makes it possible to investigate different metal-semiconductor combinations. Additionally, the flexibility of our model allows us to investigate the effect of different material properties on the quality of the contact and the nature of current flow through the contact.

V. REFERENCES

[1] K. Schauble, D. Zakhidov, E. Yalon, S. Deshmukh, R. W. Grady, K. A. Cooley, C. J. McClellan, S. Vaziri, D. Passarello, S. E. Mohney, M. F. Toney, A. K. Sood, A. Salleo, and E. Pop, "Uncovering the effects of metal contacts on monolayer MoS_2," *ACS Nano*, vol. 14, no. 11, pp. 14 798–14 808, 2020. [Online]. Available: www.acsnano.org

[2] A. V. Penumatcha, R. B. Salazar, and J. Appenzeller, "Analysing black phosphorus transistors using an analytic Schottky barrier MOSFET model," *Nat. Commun.*, vol. 6, 2015. [Online]. Available: www.nature.com/naturecommunications

[3] A. Prakash, H. Ilatikhameneh, P. Wu, and J. Appenzeller, "Understanding contact gating in Schottky barrier transistors from 2D channels," *Sci. Rep.*, vol. 7, no. 1, 2017. [Online]. Available: www.nature.com/scientificreports/

[4] S. Banerjee, L. Cao, Y. S. Ang, L. K. Ang, and P. Zhang, "Reducing contact resistance in two-dimensional-material-based electrical contacts by roughness engineering," *Phys. Rev. Appl.*, vol. 13, no. 6, p. 64021, 2020.

[5] Y. Pan, S. Li, M. Ye, R. Quhe, Z. Song, Y. Wang, J. Zheng, F. Pan, W. Guo, J. Yang, and J. Lu, "Interfacial Properties of Monolayer $MoSe_2$-Metal Contacts," *J. Phys. Chem. C*, vol. 120, no. 24, pp. 13 063–13 070, 2016. [Online]. Available: https://pubs.acs.org/sharingguidelines

[6] Á. Szabó, A. Jain, M. Parzefall, L. Novotny, and M. Luisier, "Electron Transport through Metal/MoS_2 Interfaces: Edge- or Area-Dependent Process?" *Nano Lett.*, vol. 19, no. 6, pp. 3641–3647, 2019. [Online]. Available: https://pubs.acs.org/sharingguidelines

[7] M. L. Van de Put, M. V. Fischetti, and W. G. Vandenberghe, "Scalable atomistic simulations of quantum electron transport using empirical pseudopotentials," *Comput. Phys. Commun.*, vol. 244, pp. 156–169, nov 2019.

[8] G. Bester, "Electronic excitations in nanostructures: An empirical pseudopotential based approach," *J. Phys. Condens. Matter*, vol. 21, no. 2, 2009.

[9] A. A. Laturia, M. L. Van De Put, and W. G. Vandenberghe, "Generation of empirical pseudopotentials for transport applications and their application to group IV materials," *J. Appl. Phys.*, vol. 128, no. 3, 2020.

[10] J. P. Perdew, K. Burke, and M. Ernzerhof, "Generalized gradient approximation made simple," Tech. Rep. 18, 1996.

[11] J. P. Perdew, "Density functional theory and the band gap problem," *Int. J. Quantum Chem.*, vol. 28, no. 19 S, pp. 497–523, jun 1985. [Online]. Available: https://onlinelibrary.wiley.com/doi/10.1002/qua.560280846